View metadata, citation and similar papers at core.ac.uk
brought to you by CORE
provided by Helsingin yliopiston digitaalinen arkisto

BOREAL ENVIRONMENT RESEARCH 14: 550–558
ISSN 1239-6095 (print) ISSN 1797-2469 (online)
© 2009
Helsinki 31 August 2009

Ozone concentration variations observed in northern Finland in relation to photochemical, transport and cloud processes

Tuomas Laurila, Juha-Pekka Tuovinen and Juha Hatakka

Finnish Meteorological Institute, Climate Change Research, P.O. Box 503, FI-00101 Helsinki, Finland

Received 9 Dec. 2008, accepted 27 May 2009 (Editor in charge of this article: Veli-Matti Kerminen)

Laurila, T., Tuovinen, J.-P. & Hatakka, J. 2009: Ozone concentration variations observed in northern Finland in relation to photochemical, transport and cloud processes. *Boreal Env. Res.* 14: 550–558.

Ozone concentrations measured at the Pallas-Sodankylä Global Atmosphere Watch station, located north of the Arctic Circle on a low mountain, were analysed together with data on nitrogen oxides concentrations and cloudiness. Air parcel trajectories were used to characterise the source area of air masses. The monthly mean ozone concentrations at Pallas showed a maximum in April and a broad minimum in late summer/autumn. In summer, the highest concentrations were observed in southern air masses on average, while the Atlantic and Arctic cases dominated in the earlier and latter part of the year, respectively. In autumn/early winter, there were large differences between the source areas. Throughout the year, ozone concentrations were depleted in the presence of clouds. In summer, the reduction was larger in unpolluted than polluted cases. It is suggested that the formation of nitrate radical and the scavenging of dinitrogen pentoxide act as an efficient ozone sink in winter, while in summer the difference between clear and cloudy conditions is due to the direct and indirect effects of aqueous chemistry.

Introduction

Tropospheric ozone (O_3) has raised attention in scientific community, because its present-day concentrations reach levels harmful to human health and the environment, and because it is a powerful greenhouse gas. The highly nonlinear atmospheric chemistry produces and destroys O_3, which is also transported from the stratosphere in significant amounts. As an important element of the chemical interactions, O_3 serves as the primary source of hydroxyl radical (OH), thus also affecting the oxidising and self-cleansing capacity of the atmosphere. The main characteristics of O_3 formation both in urban and background air are well known (e.g. Sillman 1999). However, there remain some poorly understood aspects of the cycling of trace gases in the troposphere, for example the chemical reactions during the polar night and in wet and cloudy environments.

In the troposphere, O_3 is formed in photochemical gas-phase reactions, in which volatile organic compounds (VOCs), methane and carbon monoxide are oxidised in the presence of catalysing nitrogen oxides (NO_x = NO + NO_2). In remote and rural areas, the rate of O_3 production depends above all on NO_x concentration (e.g. Kleinman 1994). In this process, UV radiation is necessary for the formation of OH radicals, which initiate the oxidation chains of most organic compounds. Ozone is not only formed but also consumed in the photochemical reactions. In-cloud processes are often considered

insignificant on the basis of the low solubility of O_3 in water, even though they perturb the atmospheric chemistry in a number of ways (Lelieveld and Crutzen 1991, Tost *et al*. 2007). During transport within the atmospheric boundary layer, removal by dry deposition constitutes a potentially effective sink depending on the properties of the underlying surface (Wesely and Hicks 2000). The photochemical processes responsible for O_3 formation also oxidise NO_2 to nitric acid (HNO_3), which is either taken up by aerosol particles and cloud droplets or dry deposited. In darkness, the oxidation of NO_2 by OH is not possible, and a chain of reactions involving nitrate radical (NO_3) and aqueous aerosols forms the major sink of NO_2 (Wayne *et al*. 1991). New evidence of the importance of NO_3 on nocturnal chemical processes was recently provided by Brown *et al*. (2007) and Penkett *et al*. (2007).

In Arctic conditions, with pronounced seasonal cycles of solar radiation and temperature, we may expect the processes controlling O_3 concentrations to differ substantially between the seasons. NO_x loss due to the hydrolysis of dinitrogen pentoxide (N_2O_5) dominates in winter, whereas the loss due to peroxyacetic nitric anhydride (PAN) and HNO_3 formation dominates in the spring (Stroud *et al*. 2003). Reservoir species of NO_x, such as PAN, are important in redistributing reactive nitrogen oxides, which are critical for O_3 formation. PAN was observed to be the dominant odd nitrogen species in the arctic free troposphere (Stroud *et al*. 2003). Wang *et al*. (2003) showed that there is intensive photochemical O_3 production in background air in spring, peaking in April. At mid-latitudes, the net *in situ* O_3 production can explain much of the observed column O_3 increase, although it alone cannot explain the observed April maximum. In contrast, there is a net *in situ* O_3 loss from February to April at high latitudes, and the observed continuous increase of column O_3 throughout the spring is due to tropospheric transport from other regions or the stratosphere, not *in situ* photochemistry (Wang *et al*. 2003).

Trajectory statistics show that there is efficient horizontal mixing between the high Arctic (> 80°N) and lower latitudes (Stohl 2006). The average residence time of air parcels in the lower troposphere of the high Arctic varies between one week in winter and two weeks in summer. Advection from northern Eurasia is common, but from other continental areas, especially from the high emission area of South-East Asia, isentropic and dynamic constraints limit long-range northward advection significantly. Without diabatic heating, air parcels in the atmosphere are transported along the surfaces of constant potential temperature, which has low values in the lower Arctic atmosphere. Thus the air masses originating from the low southern latitudes, where potential temperature is much higher, generally do not reach the Arctic boundary layer. Also, the potential vorticity is conserved in atmospheric motions, which restricts meridional transport over long distances. Dynamical factors may also govern the long-term changes in atmospheric concentrations. An analysis of an ensemble of long-term O_3 sounding datasets covering the Arctic showed that changes in the Arctic Oscillation (AO) explained most of the free tropospheric O_3 trend (Kivi *et al*. 2007). A possible explanation is that AO regulates the transport of O_3 and its precursors from industrialized regions towards the pole and may also modulate the stratosphere–troposphere exchange.

Transport from the stratosphere to the lower troposphere is inhibited due to the very stable stratification in the troposphere (Stohl 2006). Liang *et al*. (2008) found that it takes about three months for the stratospheric air to reach the lower troposphere. Thus the O_3 maximum in spring in the upper troposphere is associated with the flux from the stratosphere, but the peak in the lower troposphere mostly results from photochemical production. Air originating from the stratosphere is rich in nitrogen species, enhancing critically the photochemical *in situ* O_3 production in the clean parts of the troposphere (Liang *et al*. 2008).

In this study, we analyse O_3 concentrations measured in northern Finland, at a site located north of the Arctic Circle. We study the concentration variations over the seasonal cycle and analyse the relationship between O_3 and oxidised nitrogen by dividing the data into groups representing clean and polluted air masses. As our measurement site is frequently in cloud, we also investigate how the concentrations differ between cloudy and clear conditions. Further-

more, we classify our data according to the air mass source area, which we derive by analysing air parcel trajectories.

Material and methods

The measurement data we analyse were collected at the Pallas air quality monitoring station. The station is run by the Finnish Meteorological Institute and is part of the Global Atmosphere Watch (GAW) programme of the World Meteorological Organization (WMO 2001). Pallas is located in the subarctic region at the northernmost limit of the boreal zone. The mixing ratios of O_3 and NO_2 are measured on top of an Arctic mountain (Sammaltunturi, 67°58.50´N, 24°06.97´E, 565 m above mean sea level), approximately 300 m above the surrounding terrain (Hatakka *et al*. 2003). The dataset used in this study covers the period from 1 January 2000 to 31 December 2007. The auxiliary global radiation data (for 2000–2002) are from Sodankylä (67°21.71´N, 26°38.27´E), which is the other node of this GAW station.

The mixing ratio of O_3, hereafter denoted by $[O_3]$, was measured with two commercial analysers (Thermo Environmental Instruments 49C and Dasibi 1008) running in parallel. The mixing ratio of NO_2 was measured with a chemiluminescence analyser with a molybdenum converter (Thermo Environmental Instruments 42CTL). This measurement actually includes other nitrogen-containing compounds in addition to NO_2, because the molybdenum converter has a high conversion efficiency of organic nitrates and HNO_3 to NO (Fitz *et al*. 2003), which is analysed in the chemiluminescence cell. Here we designate this mixing ratio as $[NO_2^*]$. All the analysers were calibrated four times a year, the O_3 monitors against a portable calibrator and the NO_x monitor against a permeation tube for NO_2 and a calibration gas cylinder for NO.

We did not measure any speciated reactive nitrogen compounds (NO_y). However, observations from previous studies give insight on their potential contribution. According to measurements on Spitsbergen (Solberg *et al*. 1997), in winter and spring organic nitrates were the most prevalent NO_y compounds in the Arctic air. Their average mixing ratio increased from 150 pptv in early winter to a maximum of about 500 pptv in late March, and decreased thereafter. The average NO_x mixing ratio was 27 pptv and showed no clear seasonal cycle. Stroud *et al*. (2003) reported lower free-tropospheric concentrations between the latitudes of 58° and 85° in North America. In February–May, the monthly mean total $[NO_y]$ was close to 300 pptv, [PAN] was about 200 pptv, and $[NO_x]$ varied between 11 and 28 pptv. Most probably, the relative contribution of $[NO_x]$ is higher at the Pallas station, as it is located within the boundary layer and closer to populated areas.

As a component of the automatic weather station on Sammaltunturi, atmospheric visibility is measured with a Vaisala FD12P weather sensor. This sensor measures meteorological optical range (visibility) up to 50 km. According to its international definition, fog is a collection of water droplets or ice crystals that lead to a reduction of visibility to less than 1000 m (AMS 2000). We adopted the convention that the site is in cloud when visibility is less than this range, because fogs can be considered as clouds reaching the ground.

We used the deciles of $[NO_2^*]$ for classifying the data into polluted and unpolluted categories. The deciles were calculated separately for each month, with all eight years included in each monthly dataset. We graded the cases in which $[NO_2^*]$ was higher than its 90th percentile in the period in question as 'polluted'; correspondingly, the 'unpolluted' cases had $[NO_2^*]$ lower than the 10th percentile. The $[NO_2^*]$ deciles were used for dividing the $[NO_2^*]$ and $[O_3]$ data into ten groups, based on which the slope of the $[O_3]$ *vs*. $[NO_2^*]$ relationship was calculated using the least-squares linear regression technique.

The source area of air masses arriving at Pallas was determined based on air parcel trajectories. Three-dimensional trajectories ending at the 925-hPa level were calculated from the wind field data obtained from the European Centre for Medium-Range Forecasts using a kinematic trajectory model FLEXTRA (Stohl *et al*. 1999). The trajectories were generated at three-hour intervals, and their coordinates were determined backwards in time over five-day periods with a time step of one hour. Five source areas were

defined (Fig. 1), and the residence time of each trajectory in each area was recorded (Aalto *et al*. 2002). The trajectory points located beyond the map borders shown in Fig. 1 were included in the respective source area. If for some area the residence time of a trajectory was more than 50% of the total trajectory time, we allocated the observations at Pallas corresponding to the trajectory arrival time (±1 h) to that source area.

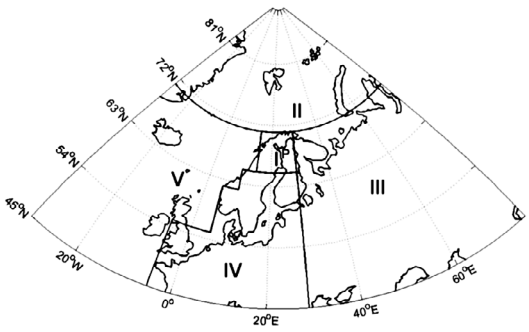

Fig. 1. Source areas used in air mass classification. I = Local, II = Arctic, III = Eastern, IV = Southern, V= Atlantic. The location of the Pallas measurement site is indicated by P.

Results

As a result of the source area analysis, 33% of all data were classified as Arctic, 17% as Atlantic, 15% as Eastern and 12% as Southern. The rest of the cases (23%) had an unclassified (mixed) source area and were not considered separately here. The monthly frequency of the Arctic class exceeded 30% during all the months except July. The Atlantic class was the most frequent one in July–August, and was also relatively common (13%–23%) throughout the year. The frequency of the Eastern cases exceeded 20% in January and November, while the Southern cases gained most importance in April (19%), but were rather infrequent in winter (within 6%–9% in January).

As shown previously (Laurila 1999, Hatakka *et al*. 2003), the highest monthly mean [O_3] was observed in April (Table 1). Except for the Arctic non-cloudy cases, this feature was independent of the air mass origin and the cloudiness conditions. However, the maximum was 3.9–5.1 ppbv lower in the air masses classified as Arctic cases compared to the other categories. The minimum in the annual cycle was broad, the monthly mean [O_3] remaining within a 3-ppbv range from July to November. The lowest mean value occurred in September, but this varied depending on the air mass origin. The Arctic cases had an earlier (July) minimum, whereas in the Southern and Atlantic cases the minimum was observed later (November and October, respectively).

In summer (June–August), [O_3] was highest in the Southern air masses, while in the earlier part of the year the highest mean [O_3] was obtained for the Atlantic subgroup of data. Correspondingly, from September to December the highest [O_3] levels were found in the Arctic air masses, and from January to March in the Atlantic air masses. Related to the different timing of the [O_3] minimum during the latter part of the year, there were significant differences in the [O_3] between the source area classes, the range of monthly average differences exceeding 10 ppbv in October–December.

The cloudy cases constituted 21.1% of the data. On a monthly basis, the frequency of these cases was highest in autumn (30% in September, 43% in October, 43% in November), and varied within 8%–20% during the other months. Both in the full dataset and in the air-mass-classified data, almost all the monthly means of [O_3] were lower for the data labelled as cloudy on the basis of poor visibility, as compared with clear conditions with visibility greater than 1 km (Table 1). The only exception was the Arctic class in April with a relatively small number of observations in cloudy conditions. The difference was largest in October–December, exceeding 10 ppbv in November. The clear/cloudy differences varied seasonally in a rather unsystematic way, except for the Arctic class, which exhibited a summer maximum. The highest difference of 15 ppbv was observed for the Eastern class in May.

The coverage of fair weather cases was very good. However, when the data were sorted according to the air mass and month, the number of cloudy cases was much smaller. To check that there were still enough independent cases, we calculated how many separate days there were in the smallest subgroups. The Arctic cloudy subgroup in August, which was the smallest subgroup, consisted of observations made in eight separate days. The other subgroups had observa-

tions from at least ten days. The lowest numbers of days with cloudy observations occurred in summer months, while the highest numbers were obtained in October–December, which months typically had about 60 separate days. On average, the monthly cloudy subgroups divided into air mass classes had 31 separate days with observations.

In winter, the mean [O_3] was clearly higher in unpolluted than in polluted cases, while the opposite was true in summer (Fig. 2). There was a steady decrease in the mean [O_3] towards the end of the summer in the clear cases, while the [O_3] measured in cloudy conditions dropped abruptly (by 18 ppbv) from April to May and thereafter remained within 21–24 ppbv until October. During this period, [O_3] was markedly smaller when a cloud was detected at the site, the monthly mean of the cloudy data being up to 15 ppbv lower than that of the rest of the data. In the polluted cases, there was a similar difference between clear and cloudy conditions. The largest differences (up to 17 ppbv in the monthly mean) took place in winter (November–January).

The range of [NO_2*] observed proves that we are in the so-called low-NO_x region. Even in the polluted cases, the monthly mean [NO_2*] was below 2.5 ppbv (Fig. 3). During the season

Table 1. Monthly global radiation sums at Sodankylä in 2000–2002 and monthly mean temperatures and ozone mixing ratios at Pallas in 2000–2007. The ozone data are presented for all air masses and the air masses dominated by different source areas. The number of cases is shown in italics.

	Jan.	Feb.	Mar.	Apr.	May	June	July	Aug.	Sep.	Oct.	Nov.	Dec.
Global radiation												
(MJ m^{-2})	5	42	163	286	397	446	389	300	147	46	9	0.5
Temperature (°C)	–10.0	–10.7	–7.5	–2.1	2.9	9.2	12.9	10.8	4.7	–1.2	–5.9	–8.4
Ozone mixing ratio (ppbv)												
All	35.9	38.4	43.6	45.3	40.4	36.2	31.3	28.9	28.5	30.6	31.1	34.3
	4009	*3688*	*4966*	*4586*	*5041*	*4580*	*4756*	*4749*	*4851*	*5489*	*4062*	*3798*
All, cloud	31.0	35.0	40.2	42.6	34.5	29.9	25.6	23.9	24.3	26.4	25.1	26.5
	788	*560*	*595*	*705*	*770*	*371*	*713*	*785*	*1472*	*2334*	*1748*	*735*
All, no cloud	37.1	39.1	44.1	45.8	41.4	36.7	32.3	29.9	30.3	33.6	35.6	36.2
	3221	*3128*	*4371*	*3881*	*4271*	*4209*	*4043*	*3964*	*3379*	*3155*	*2314*	*3063*
Arctic	38.8	41.0	43.3	42.0	37.8	34.3	26.6	28.0	30.7	34.9	36.6	37.9
	1449	*1153*	*1992*	*1414*	*1974*	*1462*	*973*	*885*	*1582*	*2060*	*1258*	*1584*
Arctic, cloud	36.9	39.3	42.2	43.2	33.0	28.2	20.3	21.3	27.8	32.2	34.7	34.9
	101	*64*	*107*	*68*	*130*	*65*	*138*	*47*	*168*	*349*	*133*	*85*
Arctic, no cloud	38.9	41.1	43.3	42.0	38.2	34.6	27.7	28.3	31.0	35.5	36.8	38.1
	1348	*1089*	*1885*	*1346*	*1844*	*1397*	*835*	*838*	*1414*	*1711*	*1125*	*1499*
Atlantic	39.0	42.4	46.5	47.2	42.9	36.9	31.8	29.3	30.1	28.7	35.2	37.5
	723	*662*	*781*	*613*	*792*	*858*	*1107*	*891*	*845*	*960*	*571*	*637*
Atlantic, cloud	33.9	38.1	42.9	45.4	39.6	32.1	29.3	25.1	24.5	24.5	30.0	30.7
	121	*103*	*70*	*60*	*49*	*48*	*40*	*82*	*153*	*352*	*197*	*96*
Atlantic, no cloud	40.0	43.1	46.9	47.4	43.1	37.2	31.9	29.7	31.3	31.1	37.9	38.7
	602	*559*	*711*	*553*	*743*	*810*	*1067*	*809*	*692*	*608*	*374*	*541*
Eastern	31.8	33.5	41.1	48.4	40.9	32.2	32.5	28.4	23.7	24.9	25.2	27.3
	812	*709*	*864*	*527*	*841*	*456*	*530*	*812*	*611*	*563*	*812*	*502*
Eastern, cloud	28.5	33.4	39.4	41.4	30.5	27.6	27.8	22.0	21.2	23.4	23.2	22.7
	245	*95*	*104*	*85*	*269*	*107*	*131*	*242*	*370*	*408*	*551*	*124*
Eastern, no cloud	33.2	33.5	41.3	49.7	45.8	33.6	34.0	31.2	27.5	29.0	29.6	28.8
	567	*614*	*760*	*442*	*572*	*349*	*399*	*570*	*241*	*155*	*261*	*378*
Southern	29.3	34.4	42.9	48.1	45.0	39.9	35.9	32.3	28.1	27.4	23.7	27.3
	229	*328*	*367*	*874*	*471*	*401*	*716*	*533*	*811*	*960*	*669*	*403*
Southern, cloud	27.2	31.4	37.6	43.1	40.8	35.5	28.6	28.5	25.8	26.0	21.0	23.1
	102	*120*	*144*	*263*	*161*	*59*	*162*	*150*	*388*	*698*	*513*	*201*
Southern, no cloud	31.0	36.1	46.4	50.3	47.2	40.6	38.0	33.8	30.2	31.0	32.5	31.5
	127	*208*	*223*	*611*	*310*	*342*	*554*	*383*	*423*	*262*	*156*	*202*

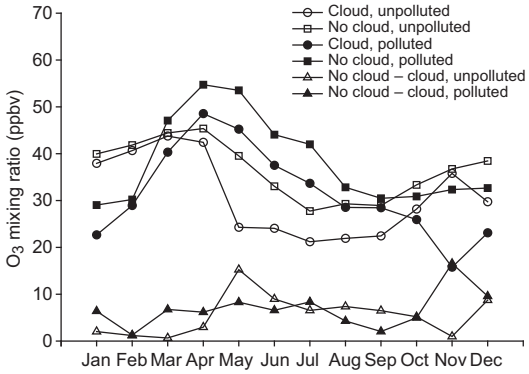

Fig. 2. Monthly mean O_3 mixing ratios in the most polluted and unpolluted air masses divided into cloudy and clear cases, and their differences.

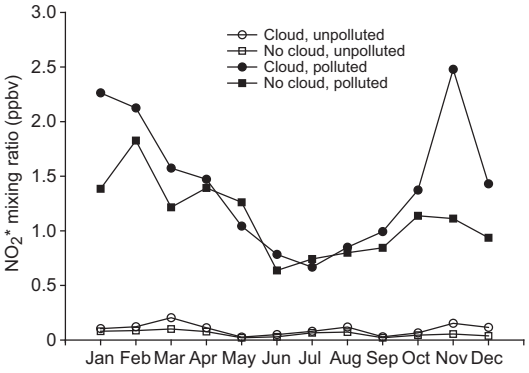

Fig. 3. Monthly mean NO_2* mixing ratios in the most polluted and unpolluted air masses divided into cloudy and clear cases.

having abundant solar radiation, [NO_2*] was less than 1 ppbv in polluted cases, and less than 0.1 ppbv in the unpolluted cases. During the season with low solar radiation levels and in polluted air masses, [NO_2*] was higher in the cloudy than clear cases. In the unpolluted cases, [NO_2*] was higher in cloudy conditions during all the seasons of the year.

The relationship between [O_3] and [NO_2*] showed consistent patterns throughout the year, following the solar radiation cycle (Figs. 4 and 5, Table 1). In winter, the slope of the linear regression (d[O_3]/d[NO_2*]) was negative, indicating that O_3 was depleted in polluted air masses. In summer, when photochemistry is active and O_3 produced, the slope was positive. This occurred from April to September.

Discussion

The high northern latitudes experience a pronounced seasonal cycle of solar radiation and temperature (Table 1) that drive many of the processes related to the tropospheric O_3 budget. At Pallas, UV radiation is practically absent in November–February. During the long dark period, chemical reactions proceed slowly, and many air pollutants, including the precursors of O_3, accumulate in the troposphere. These air pollutants act as a net sink of O_3 because, in the absence of light, O_3 is the most important oxidant. The chemical lifetime of O_3 in winter is many months (Emmons *et al*. 2003).

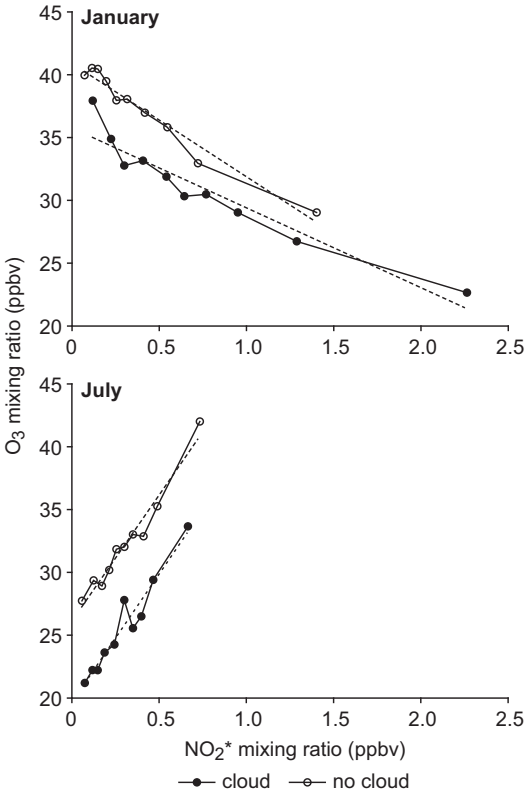

Fig. 4. Examples of the monthly relationship between [O_3] and [NO_2*] in cloudy and clear cases. Mean values of the [NO_2*] and [O_3] data, divided into ten groups on the basis of the monthly [NO_2*] deciles, are shown. The dotted lines show the linear least-square fit to the data.

The spring maximum of O_3 at Pallas is typical of remote northerly sites in Europe (e.g. Solberg *et al*. 2007). This maximum largely results from *in situ* photochemistry in the lower troposphere,

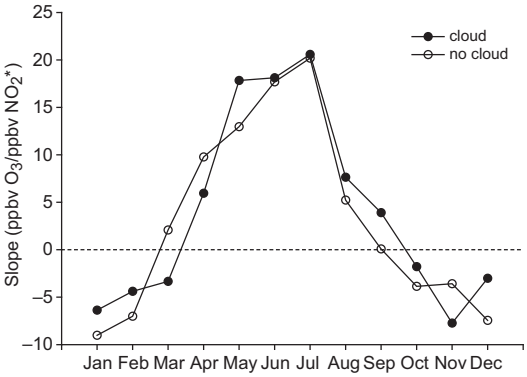

Fig. 5. Monthly slopes derived from the linear regression between $[O_3]$ and $[NO_2^*]$ in cloudy and clear cases. The regressions are based on the decile data, as shown in Fig. 4.

even though transport from the stratosphere provides upper troposphere with air rich in O_3 and NO_y species, which accelerate O_3 formation in the high-latitude upper troposphere (Liang *et al*. 2009). In the lower troposphere, only 15%–20% of O_3 originates from the stratosphere (Liang *et al*. 2009). The VOCs accumulated in winter are oxidised, enhancing $[O_3]$ on a large scale, and the long lifetime of O_3 in spring enables the long-range transport from more polluted regions (Emmons *et al*. 2003, Wang *et al*. 2003). The decline of $[O_3]$ in clean air masses after April coincides with the rapid depletion of the total reactive mass of light hydrocarbons observed at Pallas (Laurila and Hakola 1996), reflecting the transition from the photochemical processes prevailing in spring to those in summer. The enhanced dry deposition associated with the start of the growing season (e.g. Altimir *et al*. 2006) further decreases $[O_3]$ over land areas. The low correlations between $[NO_2^*]$ and $[O_3]$ in spring (Fig. 4, Hatakka *et al*. 2003) are consistent with the view that O_3 is formed slowly on a large scale (Emmons *et al*. 2003).

In autumn, concomitant to declining solar radiation, VOC concentrations start to increase (Hakola *et al*. 2006). In general, the relationship between $[O_3]$ and $[NO_2^*]$ in the monthly statistics is not clear during the spring and autumn transition months, because both O_3 production and depletion events may occur in polluted air masses, depending on the photochemical activity (Laurila 1999).

The fact that in summer $[O_3]$ is highest in the Southern air masses indicates that the contribution of the O_3 produced from European precursor emissions extends to the northern latitudes. The occurrence of the highest $[O_3]$ in the Arctic and Atlantic air masses may be related to upper tropospheric and intercontinental transport (Derwent *et al*. 2004). The seasonal $[O_3]$ cycle of the Atlantic class is very similar to that observed in unpolluted air at Mace Head on the west coast of Ireland (Simmonds *et al*. 2004).

Independent of the air mass source area, we observed a significant depletion of $[O_3]$ while a cloud was present at Pallas. Most likely these differences are generated by chemical interactions during the air mass advection to the measurement site rather than locally. The detailed mechanisms cannot be resolved from the present data, but it seems that the processes explaining this observation vary seasonally. In winter, the difference is significant only in polluted cases, in which nitrogen oxides are present. A plausible explanation would be the reaction of O_3 with NO_2 and the formation of NO_3 radical (Jacob 2000). As there is little solar radiation available, NO_3 is not photolysed but reacts with NO_2. This reaction forms N_2O_5, which is destructed by hydrolysis to HNO_3, the thermal decomposition of N_2O_5 being very slow in a cold environment. However, the gas-phase reaction of N_2O_5 with water vapour is slow too, and in order to proceed at a significant rate, the hydrolysis of N_2O_5 requires the presence of aqueous aerosols (Tie *et al*. 2003). Stroud *et al*. (2003) showed that the formation of NO_3 and N_2O_5 constitutes the main NO_x loss mechanism in the Arctic troposphere during winter until April. The rate limiting factor of this pathway is the reaction between O_3 and NO_2, if the aerosol surface area is sufficient (Tie *et al*. 2003, Stroud *et al*. 2003). This is qualitatively consistent with our observation that in the cloudy cases in winter, the depletion of $[O_3]$ is significant in polluted air masses and only marginal in unpolluted air.

In summer, the chemical reactions controlling $[O_3]$ proceed in a distinctly different way. The pathway suggested above becomes insignificant in spring with increasing radiation and temperature levels. Because of the relatively low solubility of O_3 in water, uptake by deliquesced aerosols is insignificant in cloudless conditions.

When a cloud is present, [O_3] is affected directly via aqueous-phase reactions and indirectly by modifications in the gas-phase chemistry (Lelieveld and Crutzen 1991). Peroxy radicals (HO_2 and RO_2) are highly soluble, whereas NO is not, so their reaction is insignificant in the aqueous phase, and the O_3 production efficiency in the interstitial air is reduced as the radicals are scavenged from the gas phase. In the aqueous phase, O_3 reacts with superoxide radical (O_2^-), which is replenished by uptake of HO_2 and reactions with some organic molecules, resulting in efficient destruction of O_3 (Lelieveld and Crutzen 1991). Despite the low solubility of O_3, cloud droplets can provide a locally significant sink for O_3 in cloudy areas, even if the significance of clouds may be rather limited in the larger-scale O_3 budget due to their low fraction of the total tropospheric volume (Jacob 2000).

The model simulations of Lelieveld and Crutzen (1991) indicate that in low NO_x concentrations in summer the net destruction of O_3 is significantly enhanced by clouds, whereas in higher concentrations the net photochemical O_3 production is reduced by a smaller factor. This is consistent with our data that show a large depletion effect in unpolluted air masses with NO_x mixing ratios of < 0.1 ppbv, while in polluted cases the reduction is smaller.

Conclusions

This study supports the findings that the Pallas GAW station is located in a relatively clean environment within the transition zone between the densely populated areas and the pristine Arctic. Using relatively simple chemical observations, consisting of [O_3] and [NO_2*] measured with commercial instruments, we could analyse three important processes causing O_3 variations at this site: seasonal photochemistry, air mass advection and the effect of clouds. The [O_3] data show a maximum in April and a broad minimum in late summer/autumn. The highest concentrations in summer are observed in southern air masses, while the Atlantic and Arctic cases dominate in the earlier and latter part of the year, respectively. In autumn/early winter, there are large differences between the source areas. Throughout the year, O_3 concentrations are reduced when a cloud is detected. In summer, this reduction is larger in unpolluted than polluted cases. It is suggested that the formation of NO_3 radical and the scavenging of N_2O_5 act as an efficient O_3 sink in winter, while in summer the difference between clear and cloudy conditions is due to the direct and indirect effects of aqueous chemistry. To reach more rigorous conclusions, we need more advanced measurements and cloud chemistry modelling. Future studies should also address the timescales of in-cloud processing, possibly using remote sensing data, and the effect of vertical advection.

Acknowledgements: We thank the Academy of Finland Centre of Excellence program (project nos. 211483, 211484 and 1118615) for financial support.

References

Aalto T., Hatakka J., Paatero J., Tuovinen J.-P., Aurela M., Laurila T., Holmén K., Trivett N. & Viisanen Y. 2002. Tropospheric carbon dioxide concentrations at a northern boreal site in Finland: basic variations and source areas. *Tellus* 54B: 110–126.

Altimir N., Kolari P., Tuovinen J.-P., Vesala T., Bäck J., Suni T., Kulmala M. & Hari P. 2006. Foliage surface ozone deposition: a role for surface moisture? *Biogeosciences* 3: 209–228.

AMS 2000. *Glossary of meteorology*, American Meteorological Society, Boston.

Brown S.S., Ryerson T.B., Wollny A.G., Brock C.A., Peltier R., Sullivan A.P., Weber R.J., Dubé W.P., Trainer M., Meagher J.F., Fehsenfeld F.C. & Ravishankara A.R. 2007. Variability in nocturnal nitrogen oxide processing and its role in regional air quality. *Science* 311: 67–70.

Derwent R.G., Stevenson D.S., Collins W.J. & Johnson C.E. 2004. Intercontinental transport and the origins of the ozone observed at surface sites in Europe. *Atmos. Environ.* 38: 1891–1901.

Emmons L.K., Hess P., Klonecki A., Tie X., Horowitz L., Lamarque J.-F., Kinnison D., Brasseur G., Atlas E., Browell E., Cantrell C., Eisele F., Mauldin R.L., Merrill J., Ridley B. & Shetter R. 2003. Budget of tropospheric ozone during TOPSE from two chemical transport models. *J. Geophys. Res.* 108, 8372, doi:10.1029/2002JD002665.

Fitz D.R., Bumiller K. & Lashagri A. 2003. Measurement of NO_y during SCOS97-NARSTO. *Atmos. Environ.* 37 (Suppl. 2): S119–S134.

Hakola H., Hellén H. & Laurila T. 2006. Ten years of light hydrocarbon (C_2–C_6) concentration measurements in background air in Finland. *Atmos. Environ.* 40: 3621–3630.

Hatakka J., Aalto T., Aaltonen V., Aurela M., Hakola H., Komppula M., Laurila T., Lihavainen H., Paatero J., Salminen K. & Viisanen Y. 2003. Overview of the atmospheric research activities and results at Pallas GAW station. *Boreal Env. Res.* 8: 365–383.

Jacob D.J. 2000. Heterogeneous chemistry and tropospheric ozone. *Atmos. Environ.* 34: 2131–2159.

Kivi R., Kyrö E., Turunen T., Harris N.R.P., von der Gathen P., Rex M., Andersen S.B. & Wohltmann I. 2007. Ozonesonde observations in the Arctic during 1989–2003: Ozone variability and trends in the lower stratosphere and free troposphere. *J. Geophys. Res.* 112, D08306, doi:10.1029/2006JD007271.

Kleinman L.I. 1994. Low and high NO_x tropospheric photochemistry. *J. Geophys. Res.* 99: 16831–16838.

Laurila T. 1999. Observational study of transport and photochemical formation of ozone over northern Europe. *J. Geophys. Res.* 104: 26235–26243.

Laurila T. & Hakola H. 1996. Seasonal cycle of C_2–C_5 hydrocarbons over the Baltic Sea and northern Finland. *Atmos. Environ.* 30: 1597–1607.

Lelieveld J. & Crutzen P.J. 1991. The role of clouds in tropospheric photochemistry. *J. Atmos. Chem.* 12: 229–267.

Liang Q., Douglass A.R., Duncan B.N., Stolarski R.S. & Witte J.C. 2008. The governing processes and timescales of stratosphere-to-troposphere transport and its contribution to ozone in the Arctic troposphere. *Atmos. Chem. Phys.* 9: 3011–3025.

Penkett S.A., Burgess R.A., Coe H., Coll I., Hov Ø., Lindskog A., Schmidbauer N., Solberg S., Roemer M., Thijsse T., Beck J. & Reeves C.E. 2007. Evidence for large average concentrations of the nitrate radical (NO_3) in Western Europe from the HANSA hydrocarbon database. *Atmos. Environ.* 41: 3465–3478.

Sillman S. 1999. The relation between ozone, NO_x and hydrocarbons in urban and polluted rural environments. *Atmos. Environ.* 33: 1821–1845.

Simmonds P.G., Derwent R.G., Manning A.L. & Spain G. 2004. Significant growth in surface ozone at Mace Head, Ireland, 1987–2003. *Atmos. Environ.* 38: 4769–4778.

Solberg S., Krognes T., Stordal F., Hov Ø., Beine H.J., Jaffe D.A., Clemitshaw K.C. & Penkett S.A. 1997. Reactive nitrogen compounds at Spitsbergen in the Norwegian Arctic. *J. Atmos. Chem* 28: 209–225.

Stohl A. 2006. Characteristics of atmospheric transport into the Arctic troposphere. *J. Geophys. Res.* 111: D11306, doi:10.1029/2005JD006888.

Stohl A., Haimberger L., Scheele M.P. & Wernli H. 1999. An intercomparison of results from three trajectory models. *Meteorol. Appl.* 8: 127–135.

Stroud C., Madronich S., Atlas E., Ridley B., Flocke F., Weinheimer A., Talbot B., Fried A., Wert B., Shetter R., Lefer B., Coffey M., Heikes B. & Blake D. 2003. Photochemistry in the arctic free troposphere: NO_x budget and the role of odd nitrogen reservoir recycling. *Atmos. Environ.* 37: 3351–3364.

Tie X.X., Emmons L., Horowitz L., Brasseur G., Ridley B., Atlas E., Stroud C., Hess P., Klonecki A., Madronich S., Talbot R. & Dibb J. 2003. Effect of sulfate aerosol on tropospheric NO_x and ozone budgets: model simulations and TOPSE evidence. *J. Geophys. Res.* 108, 8364, doi:10.1029/2001JD001508.

Tost H., Jöckel P., Kerkweg A., Pozzer A., Sander R. & Lelieveld J. 2007. Global cloud and precipitation chemistry and wet deposition: tropospheric model simulations with ECHAM5/MESSy1. *Atmos. Chem. Phys.* 7: 2733–2757.

Wang Y., Ridley B., Fried A., Cantrell C., Davis D., Chen G., Snow J., Heikes B., Talbot R., Dibb J., Flocke F., Weinheimer A., Blake D., Shetter R., Lefer B., Atlas E., Coffrey M., Walega J. & Wert B. 2003. Springtime photochemistry at northern mid and high latitudes, *J. Geophys. Res.* 108, 8358, doi:10.1029/2002JD002227.

Wayne R.P., Barnes I., Biggs P., Burrows J.P., Canosa-Mas C.E., Hjorth J., Le Bras G., Moortgat G.K., Perner D., Poulet G., Restelli G. & Sidebottom H. 1991. The nitrate radical: Physics, chemistry, and the atmosphere. *Atmos. Environ.* 25A: 1–201.

Wesely M.L. & Hicks B.B. 2000. A review of the current status of knowledge on dry deposition. *Atmos. Environ.* 34: 2261–2282.

WMO 2001. *Strategy for the implementation of the Global Atmosphere Watch programme (2001–2007)*. WMO TD 1077, World Meteorological Organization, Geneva.